OPEN

Oncogene (2015) **34,** 4867–4878

www.nature.com/onc

ORIGINAL ARTICLE

MicroRNA-206 functions as a pleiotropic modulator of cell proliferation, invasion and lymphangiogenesis in pancreatic adenocarcinoma by targeting *ANXA2* and *KRAS* genes

I Keklikoglou[1,2], K Hosaka[3], C Bender[1], A Bott[1], C Koerner[1], D Mitra[1], R Will[4], A Woerner[1], E Muenstermann[1], H Wilhelm[1], Y Cao[3,5,6] and S Wiemann[1]

Recent advances in cancer biology have emerged important roles for microRNAs (miRNAs) in regulating tumor responses. However, their function in mediating intercellular communication within the tumor microenvironment is thus far poorly explored. Here, we found miR-206 to be abrogated in human pancreatic ductal adenocarcinoma (PDAC) specimens and cell lines. We show that miR-206 directly targets the oncogenes *KRAS* and annexin a2 (*ANXA2*), thereby acting as tumor suppressor in PDAC cells by blocking cell cycle progression, cell proliferation, migration and invasion. Importantly, we identified miR-206 as a negative regulator of oncogenic KRAS-induced nuclear factor-κB transcriptional activity, resulting in a concomitant reduction of the expression and secretion of pro-angiogenic and pro-inflammatory factors including the cytokine interleukin-8, the chemokines (C-X-C motif) ligand 1 and (C–C motif) ligand 2, and the granulocyte macrophage colony-stimulating factor. We further show that miR-206 abrogates the expression and secretion of the potent pro-lymphangiogenic factor vascular endothelial growth factor C in pancreatic cancer cells through an NF-κB-independent mechanism. By using *in vitro* and *in vivo* approaches, we reveal that re-expression of miR-206 in PDAC cells is sufficient to inhibit tumor blood and lymphatic vessel formation, thus leading to a significant delay of tumor growth and progression. Taken together, our study sheds light onto the role of miR-206 as a pleiotropic modulator of different hallmarks of cancer, and as such raising the intriguing possibility that miR-206 may be an attractive candidate for miRNA-based anticancer therapies.

Oncogene (2015) **34,** 4867–4878; doi:10.1038/onc.2014.408; published online 15 December 2014

INTRODUCTION

Pancreatic ductal adenocarcinoma (PDAC) comprises >90% of pancreatic cancers and is one of the most deadly cancer diseases in the western world despite its comparably low incidence.[1,2] Clinical outcome is poor with only 5% of cases surviving up to 5 years after diagnosis.[1,3] PDAC arises from precursor ductal lesions termed pancreatic intraepithelial neoplasia, tends to rapidly invade in surrounding tissues, and to metastasize to other organs, primarily the liver, while it is highly resistant to chemo- and radiation therapy.[2] Hence, it is of utmost importance to fully elucidate the underlying molecular mechanisms of PDAC in order to develop novel therapeutic strategies.

One of the earliest somatic mutations in PDAC occurs in codon 12 of the *KRAS* oncogene. This results in a constitutively active KRAS protein (mostly $KRAS^{G12D}$) and is found in >90% of cases. The mutation is thought of as a key event in pancreatic intraepithelial neoplasia formation.[2,4] However, additional high-frequency genetic alterations are required to attain an invasive carcinoma phenotype. These include inactivation of tumor suppressor genes *p16INK4a/ARF* (>95%), *p53* (50–75%), *SMAD4* (55%) and *BRCA2* (5–10%).[2,5] Activated KRAS in combination with Ink4a/Arf deficiency or *PTEN* deletion are sufficient to trigger the activation of signaling circuits including the NF-κB pathway and the subsequent constitutive production of pro-inflammatory cytokines associated with vascular or immunological responses in the tumor microenvironment.[6] Indeed, it has been demonstrated that NF-κB signaling is constitutively activated in the majority of primary tumor specimens and human pancreatic cancer cell lines.[7] NF-κB has been shown to promote growth and tumorigenesis, inhibit apoptosis, as well as to foster angiogenesis, invasion, metastasis and chemoresistance in PDAC.[6,8–10]

MicroRNAs (miRNAs) are endogenous small (~22 nucleotides long) non-coding RNAs that mostly negatively regulate gene expression by base pairing within the 3′-untranslated region of target messenger RNAs (mRNA).[11] miRNAs have been well-described as regulators of many biological processes, including cancer development. Recent reports have revealed frequent alterations in miRNA expression levels also in PDAC specimens. Elevated miR-21 levels have been reported in high-grade pancreatic intraepithelial neoplasia lesions,[12] whereas high expression of miR-135b was suggested as a PDAC biomarker.[13] Here, we identify miR-206 to be significantly downregulated in tumors of PDAC patients. We reveal that miR-206 is a novel negative regulator of NF-κB signaling and, thereby, miR-206

[1]Division of Molecular Genome Analysis, German Cancer Research Center (DKFZ), Heidelberg, Germany; [2]The Swiss Institute for Experimental Cancer Research (ISREC), School of Life Sciences, Swiss Federal Institute of Technology Lausanne (EPFL), Switzerland; [3]Department of Microbiology, Tumor and Cell Biology, Karolinska Institute, Stockholm, Sweden; [4]Genomics and Proteomics Core Facility, German Cancer Research Center (DKFZ), Heidelberg, Germany; [5]Department of Cardiovascular Sciences, University of Leicester and NIHR Leicester Cardiovascular Biomedical Research Unit, Glenfield Hospital, Leicester, UK and [6]Department of Medicine and Health Sciences, Linköping University, Linköping, Sweden. Correspondence: Dr I Keklikoglou or Professor S Wiemann, Division of Molecular Genome Analysis, German Cancer Research Center (DKFZ), Im Neuenheimer Feld 580, Heidelberg 69120, Germany.
E-mail: ioanna.keklikoglou@epfl.ch or s.wiemann@dkfz-heidelberg.de
Received 2 April 2014; revised 5 October 2014; accepted 4 November 2014; published online 15 December 2014

functions as a tumor suppressor by inhibiting tumor growth, cancer cell invasiveness and release of an NF-κB-dependent circuit of pro-angiogenic cytokines and growth factors. We further demonstrate that miR-206 emerges a vascular regulatory role by leading to both vascular and lymphatic regression in PDAC tumors. Mechanistically, we propose that miR-206 exerts its tumor suppressive function through combinatorial targeting of the oncogenes *KRAS* and *ANXA2*, which, however, may have distinct roles with KRAS affecting tumor vascularization, whereas ANXA2 mainly effecting invasiveness through extracellular matrix (ECM) degradation.

RESULTS

miR-206 is downregulated in PDAC

In a previous study, we conducted a genome-wide miRNA screen, which revealed 13 miRNA families as coherent modulators of NF-κB signaling.[14] Here, in order to identify clinically relevant miRNA-NF-κB interactions in PDAC, we analyzed a publicly available miRNA expression profiling data set (GEO database—GSE32688) for differential expression of miRNAs in seven non-malignant versus 25 early stage PDAC tissues.[15] Sixty-five miRNAs were found to be significantly deregulated ($P < 0.01$) in PDAC specimens compared with healthy tissues (Figure 1a). Interestingly, miR-206, a strong negative regulator of NF-κB transcriptional activity,[14] was significantly downregulated in tumors (Figures 1a and b). miR-206 downregulation in PDAC cells was further confirmed by analyzing miR-206 expression levels in two normal and six PDAC cell lines by quantitative PCR (qPCR) (Figure 1c; Supplementary Table S1). These data suggest that miR-206 may function as a tumor suppressor in PDAC.

miR-206 exerts a tumor suppressive function in PDAC

To elucidate candidate effects of miR-206 in PDAC, miR-206 was overexpressed *in vitro* in PDAC cell lines, and alterations in cell cycle progression, cell proliferation, migration and invasion were examined. In agreement with previous studies performed in prostate and rhabdomyosarcoma cells,[16,17] miR-206 inhibited cell cycle progression in both PANC-1 and PANC10.05 cells, as ectopic expression of miR-206 led to a significant increase in the number of cells in G_0/G_1-phase compared with control cells (Figure 2a; Supplementary Figure S1b; Supplementary Table S2). Accordingly, a concomitant reduction in S- and G_2/M-phases was observed (Figure 2a; Supplementary Figure S1b). Furthermore, and in line with previous reports,[16,17] miR-206 substantially inhibited cell proliferation in a panel of pancreatic cancer cell lines (Figure 2b; Supplementary Figure S1a; Supplementary Figure S4d). Together, these results demonstrate the ability of miR-206 to cause cell cycle arrest at the G_0/G_1-phase and as such, to inhibit cell proliferation in PDAC cells.

Next, we assessed the effects of miR-206 on pancreatic cancer cell motility. Consistent with previous observations in other cancer entities,[16–18] miR-206 overexpression strongly suppressed cell migration and invasion of the highly invasive PDAC cell lines PANC-1 and BxPC-3, as determined by trans-well migration and invasion assays (Figures 2c and d). Taken together, these results indicate that the modulation of miR-206 levels impinges on cell invasion and migration in PDAC cells, thus emphasizing its tumor suppressive role in the PDAC context.

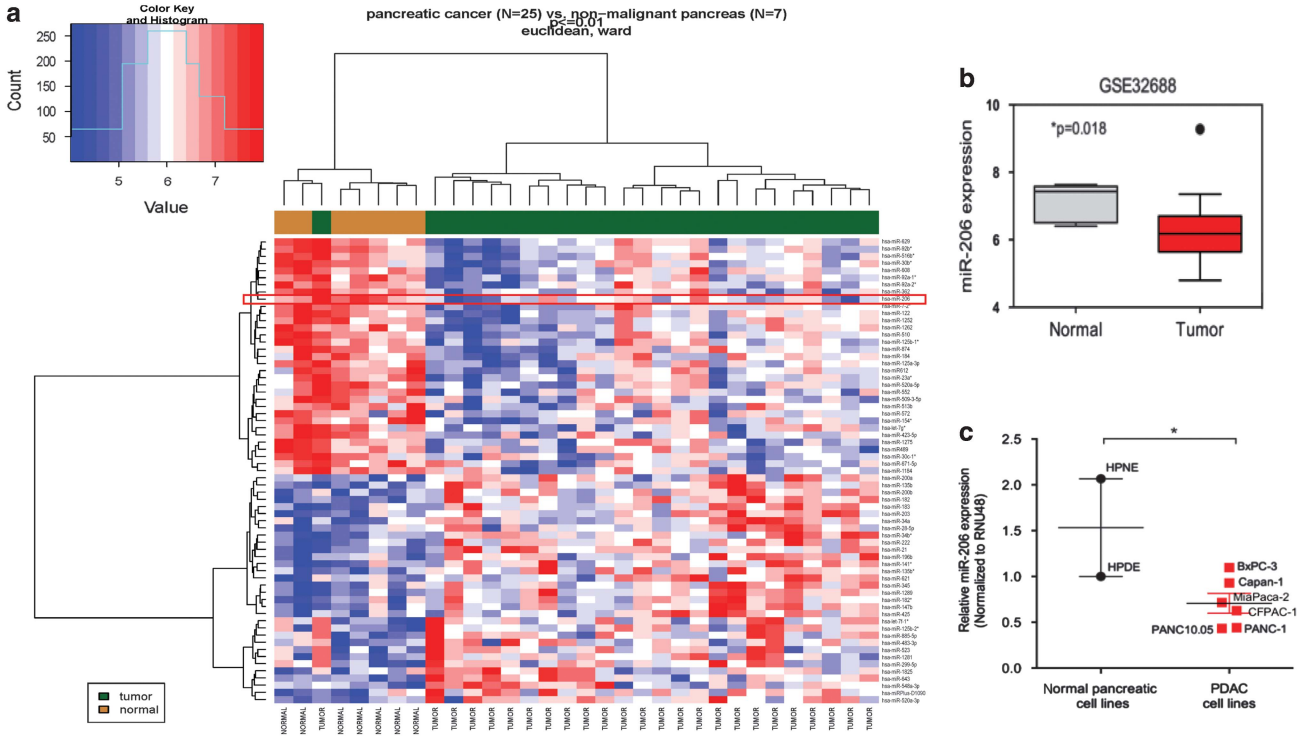

Figure 1. miR-206 is downregulated in tumor versus normal pancreatic tissue. (**a**) Heatmap visualization of differentially expressed miRNAs in 7 normal vs 25 tumor tissues of early PDAC patients (GSE32688 data set). Differential expression of miRNAs between tumor and normal samples was assessed using bioconductor's limma R-package. miRNAs with *P*-value < 0.01 (Benjamini–Hochberg corrected) were included into a heatmap visualization, using euclidean distance with the ward clustering method. (**b**) Expression of miR-206 in normal ($n = 7$) and tumor ($n = 25$) pancreatic tissues. Data represent log2 expression values. Vertical line represents the median (Whiskers: Tukey). Data were analyzed using two-tailed unpaired *t*-test (*$P = 0.018$). (**c**) Expression levels of miR-206 in normal ($n = 2$) and PDAC ($n = 6$) cell lines as determined by qPCR. Data were analyzed using two-tailed unpaired *t*-test (*$P = 0.0417$).

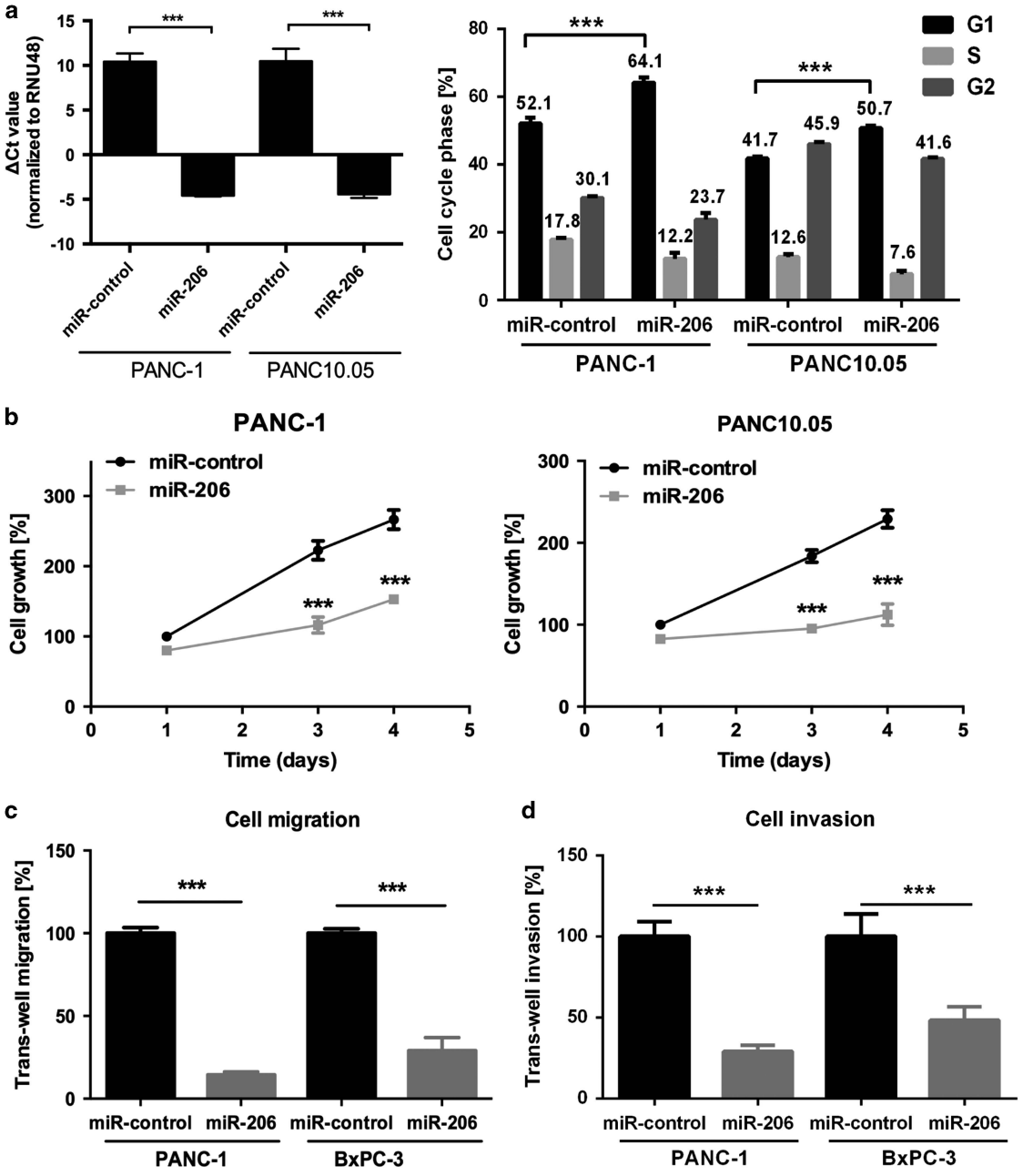

Figure 2. Expression of miR-206 alters cell cycle kinetics and suppresses cell proliferation, migration and invasion in pancreatic cancer cells. (**a**) The efficacy of miR-206 mimic overexpression in PANC-1 and PANC10.05 was determined by qRT-PCR. Cell-cycle distribution of PANC-1 or PANC10.05 cells, growing asynchronously and previously transfected with miR-206 mimic or miR-control, was measured by 7-AAD staining and quantified by flow cytometry. Experiments were performed with three replicates and in three independent experiments. (**b**) Proliferation was evaluated in PANC-1 and PANC10.05 cells for a period of 4 days, using a WST-1 assay. The measured absorbance of cells treated with the miR-control at day 1 was set at 100%. Experiments were performed with six replicates and in three independent experiments. (**c** and **d**) End point trans-well migration (**c**) and matrigel invasion (**d**) assays of PANC-1 and BxPC-3 cells transfected with microRNA mimics. Cells were transfected, seeded in 0.5% FCS medium and allowed to migrate or invade for 24 h (or 48 h in case of BxPC-3 invasion assay) using full-growth medium as chemoattractant. The number of migrated and invaded cells was quantified by flow cytometry. All experiments were performed with four replicates and in three independent experiments. Data are shown as mean ± s.d. and analyzed by a two-tailed unpaired *t*-test; $^{**}P < 0.01$, $^{***}P < 0.001$.

miR-206 inhibits NF-κB signaling and the release of pro-inflammatory and pro-angiogenic molecules in PDAC cells

NF-κB signaling is frequently constitutively activated in pancreatic cancer.[7] Indeed, the inhibition of NF-κB signaling in PANC-1 cells by using either RNA-induced knockdown of *RELA* or by proteasome (MG-132) and IκBα small molecule inhibitors (BAY-117082) led to a significant reduction of cell cycle, cell growth and migration (Supplementary Figure S2). Therefore, we assessed the ability of miR-206 to negatively regulate NF-κB activity in PDAC cells, as deregulated NF-κB signaling offers an attractive mechanistic explanation for the observed effects of miR-206 on these phenotypes. Indeed, overexpression of miR-206 resulted in a strong reduction of basal NF-κB activity, both in PANC-1 and PANC10.05 cells, and similarly also in human embryonic kidney

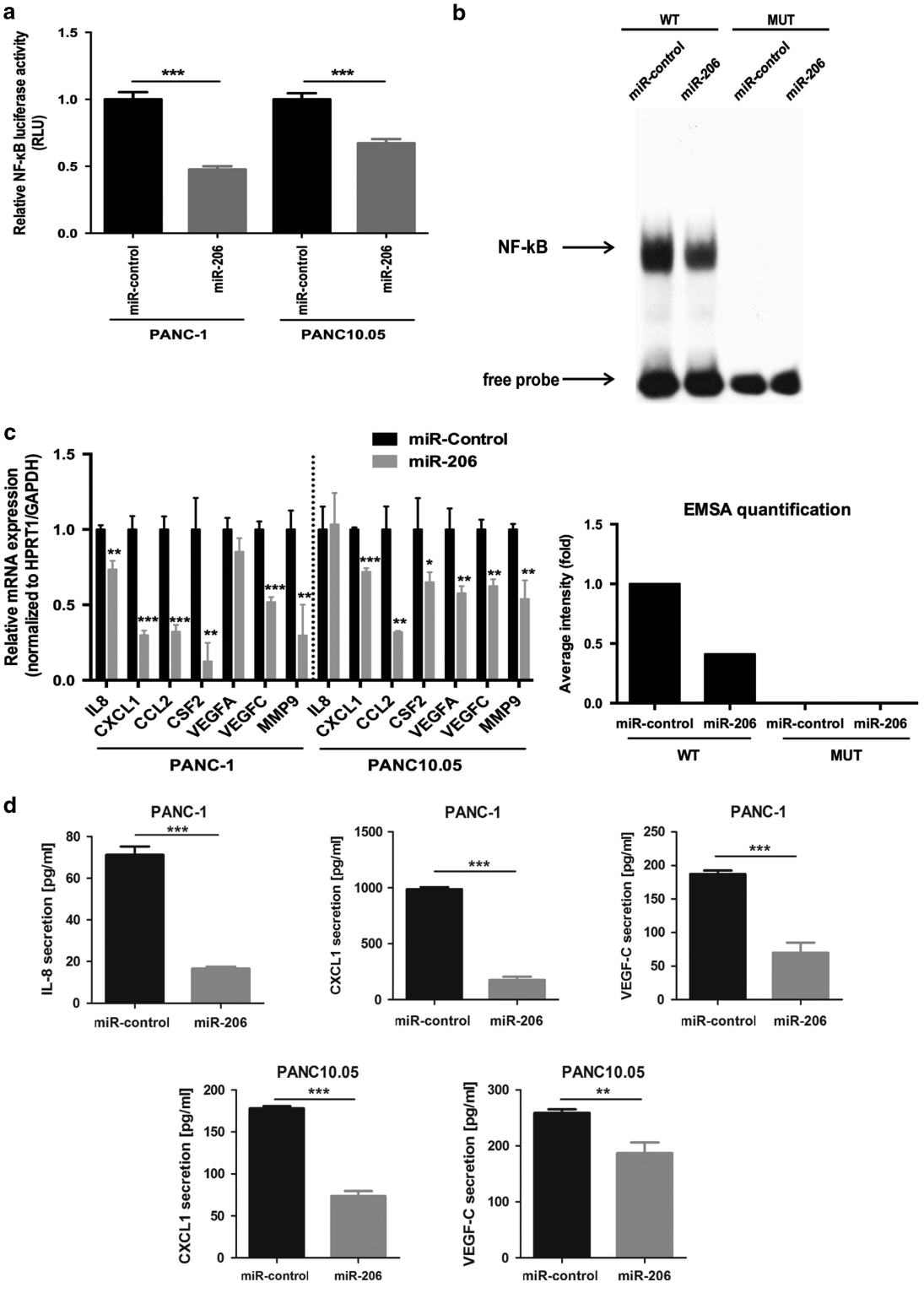

Figure 3. miR-206 negatively regulates basal NF-κB signaling and inhibits the expression of pro-inflammatory and pro-angiogenic factors in PDAC. (**a**) Basal NF-κB activity was determined in PANC-1 and PANC10.05 cells transfected with miR-206 mimic or negative control. Thirty nM of mimics, 100 ng of 3 × KBL vector and 20 ng of pMIR-β-gal were co-transfected in 96-well plate format. Forty-eight hours later, NF-κB luciferase activity was determined and normalized to the β-galactosidase activity. All experiments were performed in six replicates and data are shown as mean ± s.d. (**b**) EMSA of nuclear extracts from PANC-1 cells previously transfected with miR-206 mimic or negative control. Wild-type (WT) as well as mutated (MUT) NF-κB oligos were used as assay controls. The intensity of the bands was determined using ImageJ software. (**c**) Changes in mRNA expression levels of *IL8, CXCL1, CCL2, CSF2, VEGFA, VEGFC* and *MMP9*. PANC-1 or PANC10.05 cells transfected with miR-206 or control were assessed for changes in mRNA level of the NF-κB-dependent target genes, as determined by qRT-PCR. (**d**) VEGFC, CXCL1 and IL8 secretion (ELISA assay) in the supernatant of PANC-1 or PANC10.05 cells transfected with miR-206 mimic or negative control. All experiments were performed in triplicates and data are shown as mean ± s.d. and analyzed by a two-tailed unpaired *t*-test; $^{*}P < 0.05$, $^{**}P < 0.01$, $^{***}P < 0.001$.

cells HEK293FT (Figure 3a; Supplementary Figure S1c). Electrophoretic mobility shift assays revealed that NF-κB DNA-binding ability was reduced by approximately two fold in cells overexpressing miR-206 compared with control (Figure 3b). Collectively, these results demonstrate that miR-206 is a negative regulator of NF-κB signaling in PDAC.

As KRAS-dependent activation of NF-κB signaling supports PDAC development and progression through constitutive production of a cytokine network,[9,10,19] we next investigated whether reduced NF-κB activity caused by miR-206 would also impair the expression of validated NF-κB transcriptional target genes known to have a crucial role in modulating cancer cell motility and tumor angiogenesis. To this end, PANC-1 and PANC10.05 cell lines were used as valid models to study basal nuclear factor-κB (NF-κB) signaling because they harbor mutated *KRAS*.[20] The mRNA expression levels of several pro-inflammatory, pro-angiogenic and pro-invasive cytokines, growth factors and proteases, including interleukin-8, chemokines (C-X-C motif) ligand 1 (*CXCL1*), *CCL2* ((C–C motif) ligand 2), *CSF2* (encoding granulocyte macrophage colony-stimulating factor), vascular endothelial growth factor C (*VEGFC*) and *MMP9*, after miR-206 overexpression in PDAC cells were determined (Figure 3c; Supplementary Figure S4e;

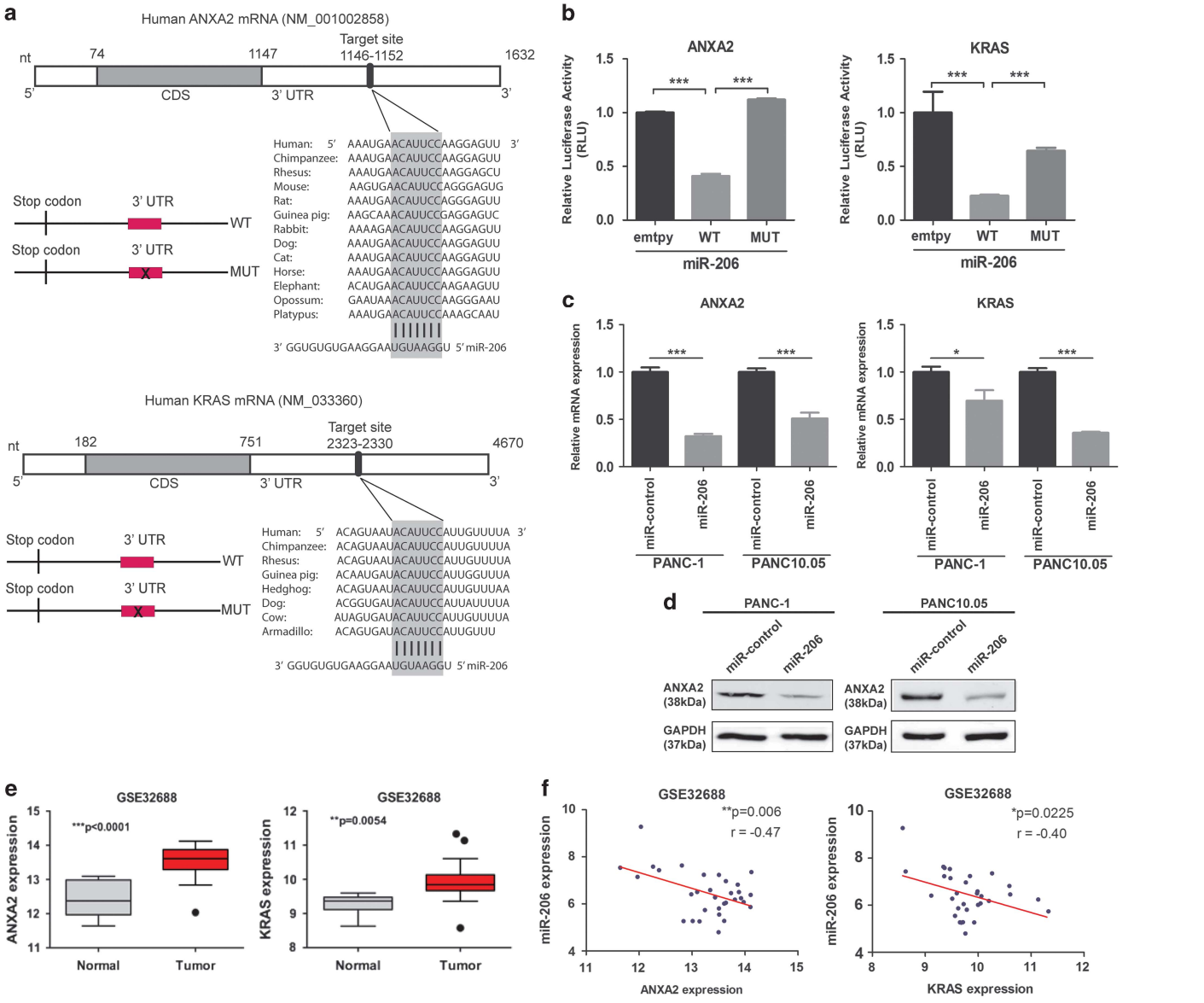

Figure 4. *ANXA2* and *KRAS* are upregulated in PDAC tumors and direct targets of miR-206. (**a**) Schematic representation of the *ANXA2* and *KRAS* mRNA with the predicted target sites for miR-206. (**b**) Luciferase reporter assay in PANC-1 cells transfected with vectors containing either the wild-type or the mutated 3′ UTRs of *ANXA2* or *KRAS* and miR-206 mimic or negative control. Experiments were performed with six replicates and data are shown as mean ± s.d. (**c**) *ANXA2* and *KRAS* mRNA levels after transfection of PANC-1 or PANC10.05 cells with miR-206 mimic or control. Total RNA was extracted 48 h after transfection and mRNA levels were determined by qRT-PCR. Experiments were performed with three replicates and in three independent experiments. Data are shown as mean ± s.d. (**d**) Total cell lysates of PANC-1 or PANC10.05 were analyzed for ANXA2 protein levels 48 h after transfection with miR-206 mimic or control by western blot. (**e**) Expression of *ANXA2* or *KRAS* in normal ($n = 7$) and tumor ($n = 25$) pancreatic tissues (GSE32688 data set). Data represent log2 expression values. Horizontal line represents the median (Whiskers: Tukey). Data were analyzed using two-tailed unpaired *t*-test, $*P < 0.05$, $**P < 0.01$, $***P < 0.001$. (**f**) Correlation analysis of miR-206 and *ANXA2* or *KRAS* mRNA expression in PDAC patients with each data point representing an individual sample and correlation coefficient (r) indicated (Pearson correlation; GSE32688 data set). Data represent log2 expression values.

Supplementary Tables S3 and S4). Indeed, miR-206 resulted in a significant downregulation of the mRNA transcripts for most of these genes in both cell lines. Interestingly, the expression of *CXCL1, CCL2, CSF2, MMP9* and *VEGFC* was reduced in both cell lines used, whereas reduced interleukin-8 expression was only observed in PANC-1 cells (Figure 3c; Supplementary Figure S4e). In accordance with these results, miR-206 strongly impaired the protein levels of CXCL1 and VEGFC in the supernatant of both cell lines, as well as of interleukin-8 in the case of PANC-1 cells (Figure 3d). To confirm that these deregulated genes are indeed NF-κB dependent in the PDAC context, we then examined their expression in PANC-1 and PANC10.05 cells after RNAi-silencing of *RELA*, the main NF-κB subunit of the canonical pathway. As expected, all genes but *VEGFC* were downregulated in cells lacking *RELA* expression compared with control cells, whereas TNF-α stimulation of PANC-1 cells induced the expression of all these genes except *VEGFC* (Supplementary Figures S3a and S3b). Hence, expression of *VEGFC* seems to be NF-κB independent in this cellular context, as inhibition of both canonical and non-canonical NF-κB members using siRNAs against *RELB* and *NFKB2* did not reduce *VEGFC* expression (Supplementary Figure S3c). Nevertheless, a direct modulation of *VEGFC* by miR-206 is rather unlikely, as *in silico* analysis (TargetScanV5.2) revealed no predicted target site within its 3′-untranslated region for miR-206. However, the molecular mechanism that leads to *VEGFC* inhibition after miR-206 overexpression remains to be elucidated.

We next recombinantly expressed RelA/p65 to potentially rescue the deregulated cytokine and pro-angiogenic factor levels in miR-206 overexpressing cells. Indeed, expression of the same cytokines and pro-angiogenic factors that we had seen to be affected by miR-206 was reinstalled when RelA/p65 was overexpressed (Supplementary Figure S3e and g), whereas only partial rescue of cell migration was observed (Supplementary Figure S3f). These data thus suggest that miR-206-induced defects on cytokine and growth factor production are driven via NF-κB signaling in PDAC cells. In contrast, the inhibitory effects of miR-206 on migration appear to only partially depend on NF-κB. Even though enhanced levels of p65 increased the number of migrated cells transfected with the miRNA-mimic-negative control, this only partially rescued the number of migrated cells overexpressing miR-206 (Supplementary Figure S3f). These findings thus suggest that expression of miR-206 negatively modulates NF-κB signaling and as such, the expression and release of pro-angiogenic and pro-invasive cytokines in PDAC.

miR-206 directly regulates *KRAS* and *ANXA2* genes

To investigate the molecular mechanism that drives miR-206 tumor-suppressing effects via blocking NF-κB pathway activation, we performed *in silico* analysis (TargetScanV5.2) for putative candidate miR-206 targets. Interestingly, *KRAS* and *ANXA2* were among the putative target genes (Figure 4a), both of which have previously been reported to be involved in NF-κB activation.[10,21] And indeed, the functionality of the predicted target sites could be validated in both genes as inhibition by miR-206 mimic was abrogated by mutations in these sites in either of the two 3′-untranslated regions (Figure 4b). In addition, overexpression of miR-206 was sufficient to inhibit endogenous mRNA expression of *KRAS* and *ANXA2* genes in PANC-1 and PANC10.05 cells (Figure 4c), as well as total ANXA2 protein levels (Figure 4d). Yet, the effects of ectopically expressed miR-206 on total KRAS protein levels could not be assessed by western blot analysis, as miR-206 led to transcriptional upregulation of *HRAS* as well as *NRAS*, both of which might cross-react with the KRAS antibody (Supplementary Figure S8). Hence, the above findings confirm that both, *KRAS* and *ANXA2,* genes are indeed novel direct targets of miR-206 in PDAC cells.

KRAS and *ANXA2* are upregulated in PDAC specimens and their expression inversely correlates with miR-206 expression

Next, in order to examine the clinicopathological relevance of the miR-206—target interaction, we analyzed *KRAS* and *ANXA2* expression in the GSE32688 data set where complementary miRNA and mRNA expression data were available. Consistent with a significantly elevated expression of *KRAS* and *ANXA2* in the tumor samples (Figure 4e), we found the same upregulation of these genes in the tumor samples of an independent data set of 45 matched normal and PDAC tissues (GSE28735)[22] (Supplementary Figure S4a). To verify that targeting of *ANXA2* and *KRAS* by miR-206 is relevant in PDAC patients, a correlation analysis between the expression levels of miR-206 and each of the two target genes was performed. Indeed, *ANXA2,* as well as *KRAS* mRNA expression was anticorrelated with miR-206 expression in PDAC specimens (Figure 4f). In summary, *ANXA2* and *KRAS* are upregulated in PDAC tumors and their negative regulation by miR-206 is clinically relevant in the context of PDAC.

miR-206 impairs NF- κB signaling via negative regulation of KRAS

As both, KRAS[10] and ANXA2,[21] have been implicated with NF-κB activation, we next investigated whether the inhibition of KRAS and/or ANXA2 could mechanistically explain the observed effects of miR-206 in PDAC cells. First, the basal NF-κB pathway activity was determined after silencing the *KRAS* and *ANXA2* genes in PANC-1 cells (Figure 5a; Supplementary Figure S5; Supplementary Table S5). As expected, silencing of *KRAS* with either of the two siRNAs used significantly reduced NF-κB luciferase activity compared with control cells; however, RNAi-induced knockdown of *ANXA2* did not alter the basal NF-κB activity (Figure 5a; Supplementary Figure S5c). These findings suggest KRAS as a mechanistic link between miR-206 and NF-κB pathway inhibition. Next, we assessed whether targeting of *KRAS* mediates the reduction of the NF-κB-dependent target genes that were downregulated upon miR-206 overexpression (Figure 3b) in PDAC cells. Notably, silencing of *KRAS* led to a stringent downregulation of interleukin-8, *CXCL1* and *CSF2* transcripts in PANC-1 cells, whereas it abrogated *CSF2* and *VEGFA* mRNA expression in PANC10.05 cells compared with control siRNA-transfected cells (Figure 5b). Hence, the above findings suggest that decreased pro-inflammatory and pro-angiogenic cytokine production by PDAC cells upon miR-206 overexpression could be attributed to direct targeting of *KRAS*, at least in part.

miR-206 controls PDAC cell growth, migration and invasion through *ANXA2* and *KRAS* targeting

We then assessed if targeting of *KRAS* and/or *ANXA2* would phenocopy miR-206-induced phenotypes on cell proliferation, migration and invasion. Indeed, we observed a cell cycle arrest in G_0/G_1- and G_2-phases after silencing of *KRAS* or *ANXA2* in PDAC cells, respectively (Figure 5c). This was accompanied by reduced cell viability (Figure 5d). Furthermore, silencing of either *ANXA2* or *KRAS* decreased the number of migrated and invaded PANC-1 cells (Figures 5e and f). In line with earlier observations,[23,24] silencing of *ANXA2* abrogated the invasive capacity of BxPC-3 cells, which harbor wild-type KRAS; however, RNAi-induced knockdown of *KRAS* did not alter the number of invaded BxPC-3 cells (Figure 5f). Collectively, these results suggest that miR-206 inhibits PDAC cell proliferation, migration and invasion, through combinatorial targeting of *ANXA2* and *KRAS*.

As ANXA2 has been shown to facilitate plasmin generation resulting in degradation of the extracellular matrix and subsequent cell invasion, we reasonably asked if the effect of miR-206 on cancer cell invasion is mediated by reduced ANXA2-dependent plasmin production. To this end, cells were transfected with miR-206 mimic, siANXA2 or respective controls and 48 hours later

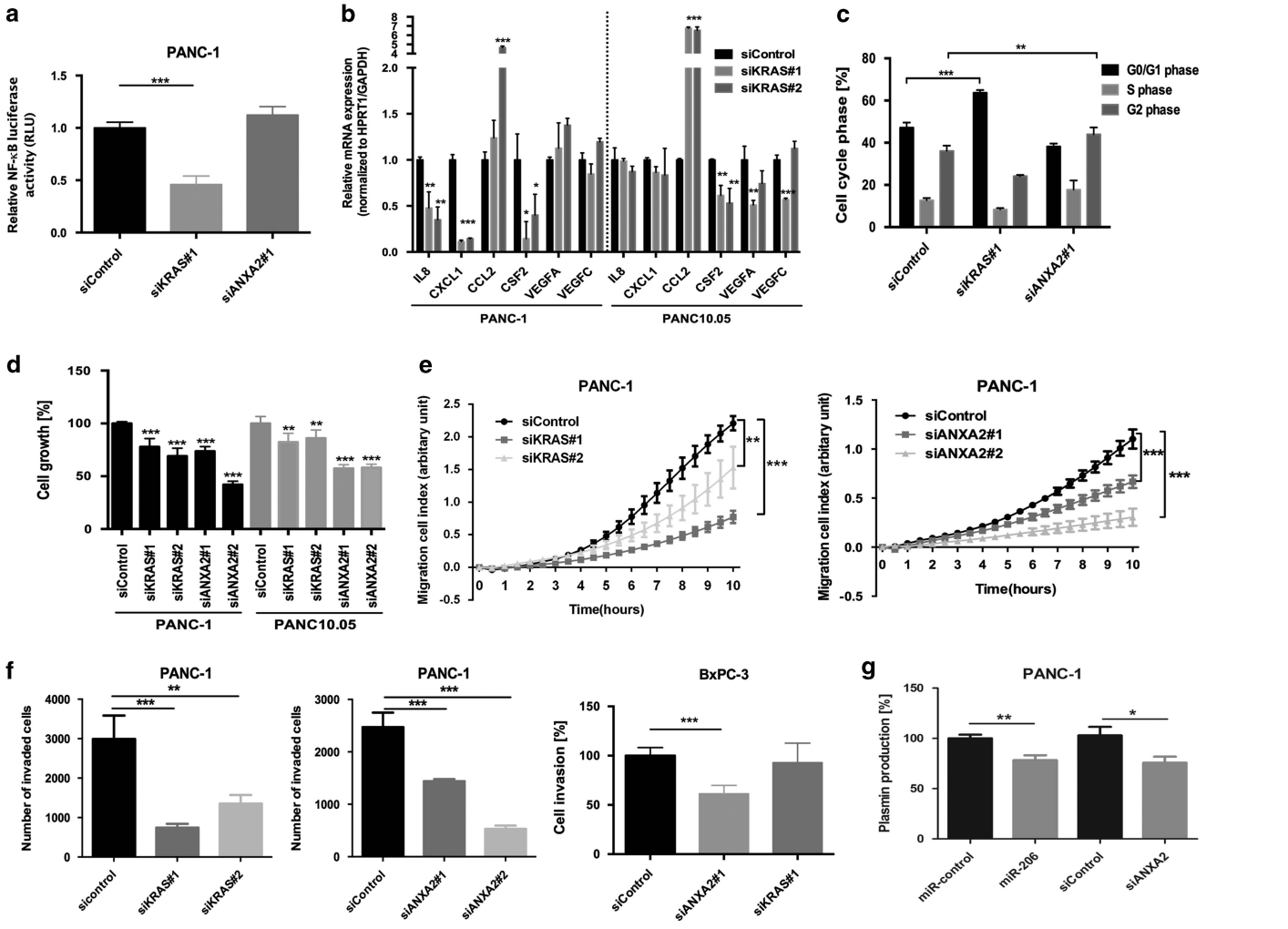

Figure 5. Inhibition of *KRAS* and *ANXA2* oncogenes mediates the observed miR-206 phenotypes in PDAC cells. (**a**) Basal NF-κB activity was determined in PANC-1 cells transfected with siRNAs against *KRAS*, *ANXA2* or non-targeting control. NF-κB luciferase activity was normalized to the β-galactosidase activity. The experiment was performed with six replicates and in three independent experiments. (**b**) PANC-1 and PANC10.05 cells transfected with two individual siRNAs against *KRAS* or control were assessed for changes in mRNA level of the *IL8, CXCL1, CCL2, CSF2, VEGFA* and *VEGFC* genes as determined by qRT-PCR. The experiment was performed in triplicates and in three independent experiments. (**c**) Cell-cycle distribution of PANC-1 cells, previously transfected with siKRAS, siANXA2 or negative control, and growing in full-growth medium for 72 h was measured by 7-AAD staining and quantified by flow cytometry. Experiments were performed with three replicates. (**d**) Proliferation was evaluated in PANC-1 and PANC10.05 cells 3 days after transfection with two individual siRNAs against either *KRAS* or *ANXA2* genes, using a WST-1 assay. Cell viability experiments were performed with six replicates and in three independent experiments. (**e**) Cell migration of PANC-1 cells previously transfected with two individual siRNAs against either *ANXA2* or *KRAS*, as well as with the negative control was assessed by an RTCA (real-time cell analyzer) trans-well migration assay. Cells were seeded in 0.5% FCS medium and allowed to migrate for 10 h using full-growth medium as chemoattractant. Impedance measurements were performed in a time-resolved manner. Means of four replicates ± s.d. are shown; a two-tailed upaired *t*-test was performed for the last time point. (**f**) End point matrigel invasion assay of PANC-1 and BxPC-3 cells transfected with siRNAs against either *ANXA2* or *KRAS*, as well as with the negative control. Cells were transfected, seeded in 0.5% FCS medium and allowed to invade for 24 h (or 48 h in case of BxPC-3 cells) using full-growth medium as chemoattractant. The number of invaded cells was quantified by flow cytometry. Experiments were performed with four replicates and in three independent experiments. Data are shown as mean ± s.d. (**g**) Plasmin production (activity) was determined in PANC-1 cells previously transfected with miR-206 mimic, siANXA2 or control. Cells were treated with t-PA (10 μg/ml), 0.4 μM of plasminogen and 10 μl of the plasmin substrate (Spectrozyme). Produced active plasmin was determined by measuring absorbance at 405 nm. Experiments were performed with four replicates and in three independent experiments. Data are shown as mean ± s.d. All data were analyzed by a two-tailed unpaired *t*-test; $^{*}P < 0.05$, $^{**}P < 0.01$, $^{***}P < 0.001$.

plasmin (Pm) generation from plasminogen (Pg) was measured. As expected, both miR-206 overexpression as well as silencing of *ANXA2* led to a significant reduction of plasmin activity on the cell surface of PANC-1 cells (Figure 5g). Together, these results demonstrate that miR-206 inhibits cancer cell invasion through multiple oncogenic routes involving targeting of *ANXA2*, and this effect can be attributed mechanistically to reduced ANXA2-dependent plasmin production.

miR-206 delays tumor growth in PDAC xenografts

Having collected a large body of evidence that miR-206 is capable of impacting tumor phenotypes *in vitro*, we were next out to study the biological function of miR-206 in PDAC tumors *in vivo*. To this end, we generated a PANC10.05 cell line stably overexpressing human miR-206 using the retroviral pBABE vector system for cell transduction (Figure 6a). These pBABE-miR-206 PANC10.05 cells or control cells transduced with empty vector (pBABE-empty) were

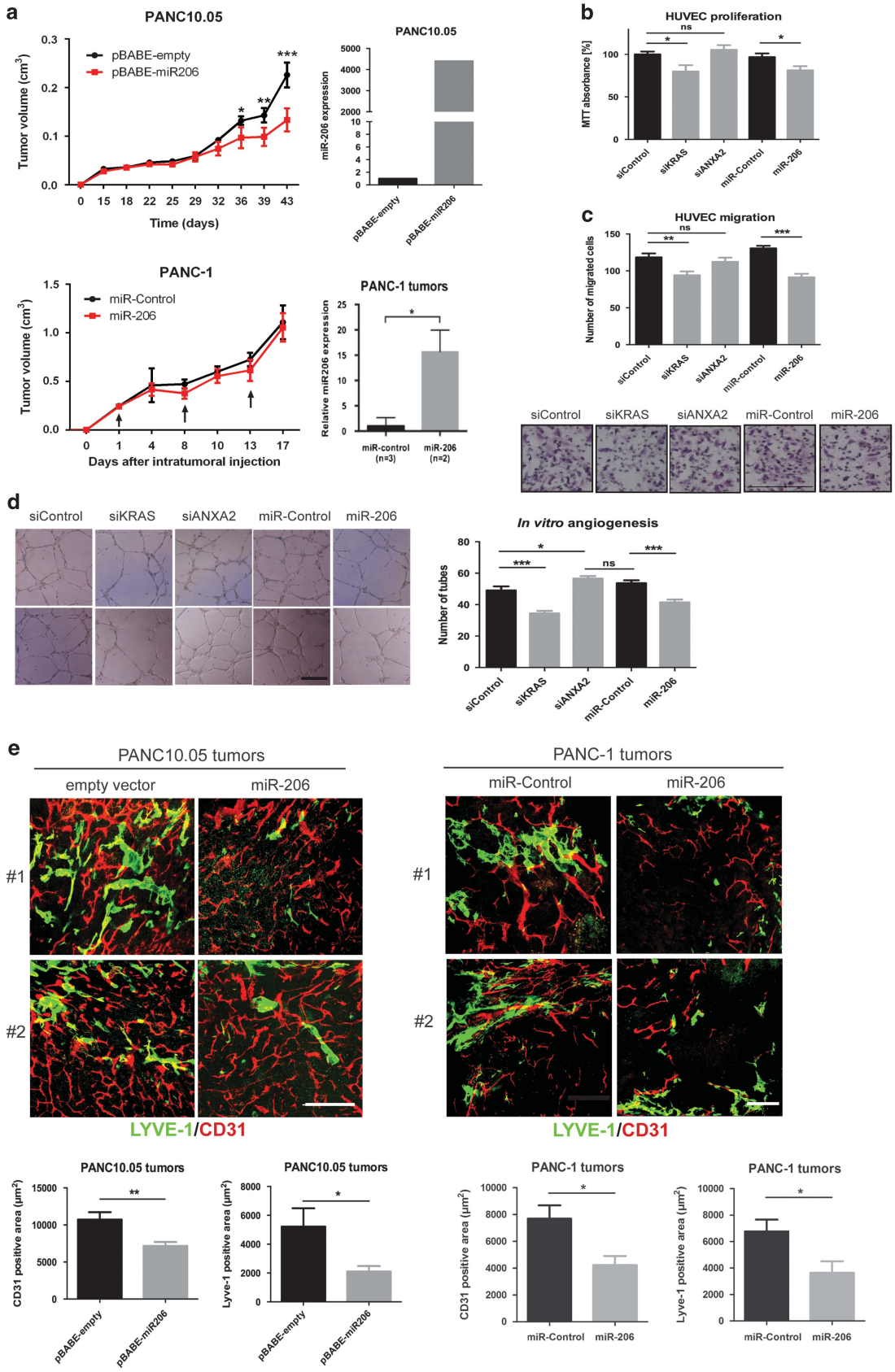

subcutaneously injected into the back along the mid-dorsal line of severe combined immunodeficiency (SCID) mice ($n = 7$ mice per group). In agreement with our *in vitro* findings, tumors derived from pBABE-miR-206 PANC10.05 cells grew significantly slower than tumors derived from pBABE-empty control cells (Figure 6a). As the generation of PANC-1 cells stably overexpressing miR-206 was not feasible because miR-206 expression was silenced by endogenous cell mechanisms as soon as 1 week after transduction, we used synthetic miR-206 mimics *in vivo* to test the therapeutic potential in this cell line. To this end, untreated PANC-1 cells were subcutaneously injected in SCID mice and maintained until the cells had formed palpable tumors with an average volume of 0.2 cm^3 ($n = 5$–6 mice per group). Tumors were then repeatedly injected intratumorally with miR-206 or negative control-miRNA in collagenase solution, once a week. All mice were killed 7 days after the last injection, tumors were harvested and miR-206 *in vivo* transfection efficiency, as well as miR-206-induced targeting of *KRAS* and *ANXA2* were verified by qPCR (Figure 6a; Supplementary Figure S6c). Although we did not observe an effect on the tumor burden after miR-206 treatment, these tumors presented massive tumor necrosis compared with tumors treated with negative control (Supplementary Figure S6). Together, the above findings demonstrate that elevated expression of miR-206 may dampen PDAC tumor growth.

miR-206 blocks tumor lymphangiogenesis and angiogenesis *in vitro* and *in vivo*

As miR-206 overexpression was sufficient to inhibit the production of several pro-angiogenic and/or pro-lymphangiogenic factors, we next asked whether miR-206 would impair tumor vascularization and/or lymphangiogenesis. To this end, we assessed the ability of cancer cell-derived factors regulated by miR-206 to impact on endothelial physiology *in vitro* through alterations in the downstream cytokine network. Indeed, human vein endothelial cells (ECs) treated with conditioned medium from miR-206-transfected PANC-1 cells displayed reduced proliferation and migration rates compared with control treated cells (Figures 6b and c). Similarly, silencing of *KRAS* but not of *ANXA2* phenocopied the observed miR-206 effects on angiogenic response of these cells (Figures 6b and c). Next, we wanted to learn to what degree the secreted factors from miR-206 transfected cancer cells would induce the formation of capillary-like tubes. Human vein ECs were seeded on matrigel in the presence of conditioned medium from miR-206-transfected PANC-1 cells. As expected, the number of capillary-like tubes was reduced in the presence of miR-206 conditioned medium (Figure 6d). A concomitant reduction in tube-like structures was observed also with conditioned medium from PANC-1 cells where *KRAS*, but not *ANXA2*, had been silenced (Figure 6d).

To verify our findings also *in vivo*, we analyzed miR-206 overexpressing PANC-1 and PANC10.05 tumors (Figure 6a) for vascular and lymphatic density by whole-mount staining. Of note, miR-206 overexpression reduced tumor vascularization as determined by quantification of anti-CD31 staining (Figure 6e). Furthermore, a striking reduction in the intratumoral lymphatics coverage was observed in both miR-206 overexpressing tumor models compared with control tumors, using an anti-LYVE-1 antibody (Figure 6e). Taken together, the above findings demonstrate a vascular regulatory role for miR-206 in PDAC tumors.

DISCUSSION

Here we show that downregulation of miR-206 in PDAC is important for cancer cells to sustain their invasive and proliferative capacities, as re-expression of miR-206 in PDAC cells strongly inhibited both cell invasion and cell growth. Mechanistically, we could link defects in cell viability and motility to the direct targeting of oncogenic *KRAS*, an upstream regulator of NF-κB signaling,[10] and of *ANXA2,* which is a major regulator of ECM degradation.[25,26]

Nevertheless, the molecular mechanisms that lead to loss of miR-206 expression in human cancers are not yet fully elucidated. In cancer cells, it is plausible that miR-206 is silenced by epigenetic modifications (that is, promoter hypermethylation).[16] Intriguingly, a recent study revealed that in lung cancer, miR-206 is negatively regulated by nuclear factor erythroid-2-related factor 2, a transcription factor, which is critical for sustaining tumor growth through glucose metabolism reprogramming.[27] Although such epigenetic or molecular regulation of the miR-206 in PDAC is possible, the exact mechanism that leads to its suppression in this cancer type needs further investigation.

Our study shows that miR-206 negatively regulates *in vitro* EC proliferation, migration and capillary-like tube formation, as well as *in vivo* tumor angiogenesis and lymphangiogenesis by modulating a pro-angiogenic cytokine network, the majority of which is under NF-κB transcriptional control. Importantly, we identified *CSF2*, *CXCL1*, *IL8*, *CCL2* and *VEGFC* expression to be abrogated upon miR-206 expression. Indeed, the chemokines CXCL1 and IL8 have long been thought as major pro-angiogenic factors as they trigger EC proliferation, migration and, hence, accelerate tumor vascularization and growth.[27–30] Apart from its pro-angiogenic activity,[31] oncogenic KRAS-induced granulocyte

Figure 6. miR-206 inhibits *in vitro* angiogenesis and *in vivo* tumor growth, angiogenesis and lymphangiogenesis in PDAC xenografts. (**a**) *in vivo* tumor growth after re-expression of miR-206 was monitored in PDAC xenograft mouse models. PANC10.05 cells stably overexpressing miR-206 (pBABE-miR-206) or the control vector (pBABE-empty) were injected subcutaneously into the back along the mid-dorsal line of SCID mice ($n = 7$ in case of pBABE-empty and $n = 8$ in case of pBABE-miR-206 tumors). Tumor volume was measured every 2–3 days for 43 days after inoculation. Stable overexpression of miR-206 in PANC10.05 cells was validated by qRT-PCR. Established tumors from PANC-1 cells that were injected s.c. into the back along the mid-dorsal line of SCID mice were randomized into two groups when tumor size reached a size of 0.2 cm^3 and were subsequently transfected *in vivo* weekly with a mixture of miR-206 mimics ($n = 6$) or miRNA-negative control ($n = 5$) in 0.015% collagenase II solution intratumorally. The arrows indicate each intratumoral miRNA injection. Tumor volumes were measured for 17 days after the first intratumoral miRNA injection. All mice were killed 7 days after the last injection. *In vivo* miRNA transfection efficiency was determined by quantifying miR-206 levels in dissected PANC-1 tumors by qRT-PCR. Data are shown as mean ± s.e.m. (**b**) HUVEC cell proliferation in the presence of conditioned medium derived from PANC-1 cells previously transfected with siRNAs against either *ANXA2* or *KRAS*, as well as with miR-206 mimics or negative controls ($n = 6$/group) was determined after 72 h by MTT assay. Data are shown as mean ± s.e.m. (**c**) HUVEC cell trans-well migration towards conditioned medium derived from PANC-1 cell previously transfected with miRNA mimics, siRNAs or controls ($n = 6$/group) was evaluated by light microscopy. Cells were counted and data are shown as mean number of counted cells/field ± s.e.m. Scale bar, 250 μm. (**d**) Capillary-like tube formation was determined using HUVEC cells treated with conditioned medium of PANC-1 cells previously transfected with either siRNAs or miRNA mimics for 6 h ($n = 6$/group). Data are shown as mean number of tubes/field ± s.e.m. Scale bar, 250 μm. (**e**) Whole-mount staining of PANC-1 and PANC10.05 tumors overexpressing miR-206 or negative control for CD31 and LYVE-1 stainings. Scale bar for PANC10.05 and PANC-1 tumors is 50 μm. The quantification of angiogenesis and lymphangiogenesis was determined by calculating the mean of the total area of CD31 and LYVE-1 positive area (μm2) per field ± s.e.m., respectively ($n = 6$–9/group). Data were analyzed by a two-tailed unpaired *t*-test; $^*P < 0.05$, $^{**}P < 0.01$, $^{***}P < 0.001$.

macrophage colony-stimulating factor production is required for intrapancreatic recruitment and accumulation of immunosuppressive $Gr1^+CD11b^+$ myeloid cells and as such, is necessary for PDAC progression and tumor growth.[32] Intratumoral accumulation of $Gr1^+CD11b^+$ cells may promote angiogenesis through secretion of MMP9,[33] thus leading to release of potent angiogenic factors, such as VEGF, that are usually sequestered in the ECM.[34] Similarly, CCL2 has been recently described as a pro-angiogenic and pro-inflammatory factor, as it can stimulate ECs to initiate an angiogenic program either directly[35] or indirectly through intratumoral macrophage/monocyte recruitment.[36] It is thus plausible that miR-206 may modulate tumor vessel formation also indirectly by dampening immune cell infiltration. However, as there is no miR-206 target site in murine *KRAS*, we lacked the possibility of using syngeneic mouse models to study the cross-talk of the aforementioned cancer cell-derived factors with inflammatory cells. Hence, we restricted ourselves in studying the direct effects of these factors to the ECs, using PDAC xenografts. In agreement with our findings, it has been recently reported that miR-206 modulates vasculature formation during developmental angiogenesis via VEGFA targeting.[37] Indeed, we observed a significant reduction of secreted VEGFA from PDAC cells overexpressing miR-206 (Supplementary Figure S7). Hence, miR-206 may modulate tumor vascularization via multiple cytokine networks.

Importantly, our study is the first to place miR-206 as a novel anti-lymphangiogenic factor by inhibiting *VEGFC* expression, a potent regulator of tumor lymphangiogenesis.[38–40] Although in normal conditions the physiological role of the lymphatic system is to maintain tissue-fluid homeostasis and immune cell trafficking, in cancer, invasive cancer cells use the blood and the lymphatic vessels to spread and metastasize to lymph nodes and distant organs.[39,41] Thus, normalization of tumor-associated blood and lymphatic vasculature is highly needed to succeed tumor shrinkage, inhibition of metastasis and efficient intratumoral drug and cytotoxic leukocyte systemic delivery during anticancer therapy. Hence, the ability of miR-206 to attenuate tumor vascularization is highly attractive.

We further demonstrate that miR-206 inhibits the invasive capacity of PDAC cells through combinatorial targeting of *ANXA2* and *KRAS* genes. Importantly, targeting of *ANXA2* reduced plasmin production on the PDAC cell surface, suggesting miR-206 as a novel regulator of ECM degradation. In agreement with our findings, ANXA2 has been recently shown to be upregulated in many tumor entities including lung and breast cancer,[42,43] whereas its expression correlates with poor prognosis in multiple myeloma and pancreatic cancer.[24,44] Our study provides a miRNA-mediated mechanistic explanation for ANXA2 upregulation in PDAC tumors, as it comprises a clinically relevant miR-206 target. Although a pro-angiogenic role for ANXA2 has been recently described,[42] we did not observe any effect on *in vitro* EC proliferation, migration or tube formation in the presence of conditioned medium of PDAC cells when *ANXA2* had been silenced. However, it is possible that *ANXA2* targeting may contribute to neovascularization through proteolytic ECM remodeling, thus allowing ECs to transmigrate and proliferate in the perivascular tissue.[45] Although miR-206 has been discussed as a potential tumor suppressor,[16–18,46] we here demonstrate that the expression of miR-206 is abrogated in PDAC and we present data explaining the molecular mechanisms of its activity.

In summary, we provide a new understanding of the roles miR-206 has in PDAC by providing evidence of its diverse functions. In particular, we show that miR-206 regulates different hallmarks of cancer,[47] including cell proliferation, invasion, and tumor angio- and lymphangiogenesis through combinatorial targeting of multiple oncogenic routes, involving KRAS-induced NF-κB signaling, the pro-metastatic gene *ANXA2* and the potent pro-lymphangiogenic factor VEGFC (Figure 7). Hence, these findings may have important translational implications, as a miR-206-based therapy might be an attractive therapeutic strategy to treat PDAC.

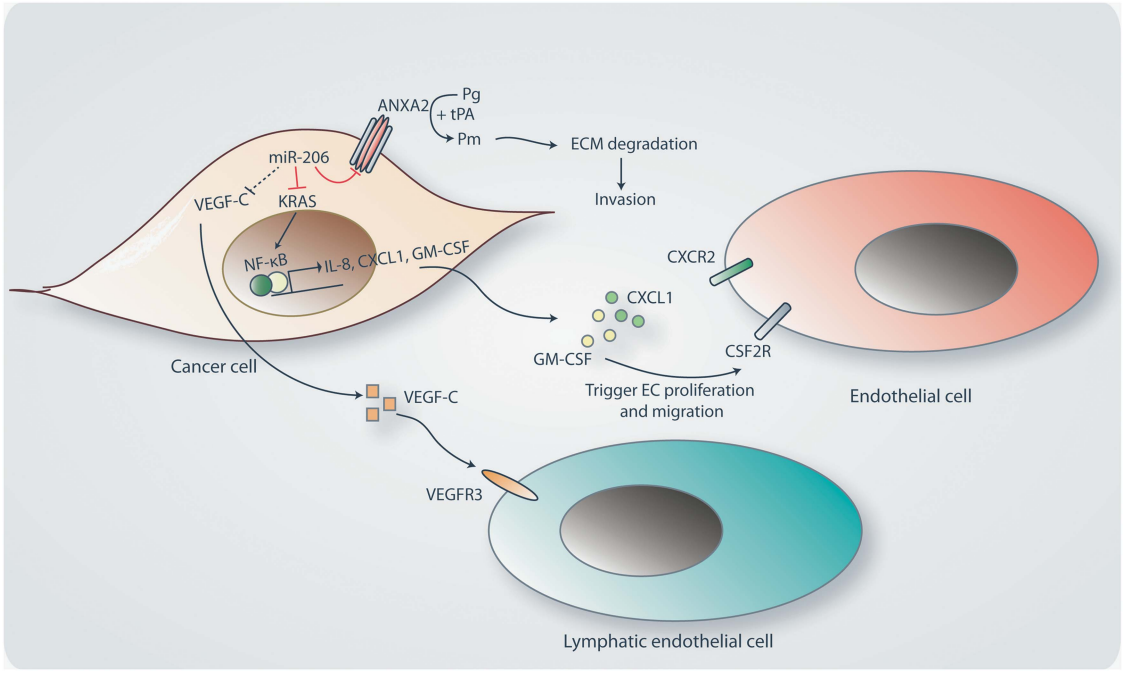

Figure 7. Schematic representation of the miR-206 proposed mode of action in modulating PDAC tumor responses. miR-206 functions as a tumor suppressor in PDAC cells by directly dampening the antiapoptotic KRAS-induced NF-κB pathway activity, thus leading to transcriptional inhibition of the expression of multiple pro-angiogenic, pro-lymphangiogenic and growth factors, thus limiting endothelial (EC) and lymphatic endothelial cell activation and tumor growth. In addition, miR-206 inhibits ECM remodeling by directly targeting ANXA2, which serves as a proteolytic center for ECM degradation.

MATERIALS AND METHODS

Cell lines and transfection reagents

PANC-1 and PANC10.05 cell lines were obtained from the American Type Culture Collection (ATCC, Manassas, VA, USA). BxPC-3, MiaPaca-2, CFPAC-1, Colo357 and Capan-1 cell lines were provided by Dr Joerg Hoheisel and HPNE and HPDE cell lines were provided by Dr Christoph Roesli (both DKFZ, Heidelberg). HEK293FT cells were obtained from Invitrogen (Carlsbad, CA, USA). All cell lines used were tested for Mycoplasma infection and were verified for authenticity (DKFZ core facility). PANC10.05 cells stably overexpressing miR-206 were generated using the pBABE-puro retroviral system. The pre-miR-206 sequence along with 300 nucleotide-long flanking sequence was cloned into pBABE-puro vector using *Bam*HI and *Xho*I restriction enzymes. PANC10.05 cells were transduced with pBABE-empty (control) or pBABE-miR-206 and selected in 2 mg/ml puromycin (Invitrogen).

Transfections were performed using using Lipofectamine 2000 (Invitrogen) according to the manufacturer's instructions. All siRNAs, as well as the non-targeting control siRNA, were from Ambion (Austin, TX, USA). The second siRNA against *ANXA2* gene (siANXA2#2) was from Dharmacon (Lafayette, CO, USA). For each gene, 2 individual siRNAs were used (Supplementary Table S6). miRIDIAN miRNA mimics and the negative control were obtained from Dharmacon. siRNAs and miRNA mimics were used at a final concentration of 30 nM, unless mentioned differently.

Luciferase assays

Luciferase reporter assays were performed as previously described.[14]

Plasmin production assay

Transfected PANC-1 cells were trypsinized and re-seeded on 24-well plates (100 000 cells/well) in full-growth medium. Twenty-four hour later, cells were detached using an enzyme-free dissociation solution (Sigma-Aldrich, Saint-Louis, MO, USA). Cells were centrifuged for 4 min at 2500 rpm and the cell pellet was washed with 1 × phosphate-buffered saline (PBS). To trigger plasmin (Pm) production from plasminogen (Pg), t-PA (Sigma-Aldrich) was added in a concentration of 1 μg/ml, diluted in PBS. Then, cells were incubated on ice for 30 min, washed with 1 × PBS, and 0.4 μM glu-plasminogen (American Diagnostica, Pfungstadt, Germany) were added in 100 μl of PBS together with 10 μl of Spectrozyme (American Diagnostica). Plasmin production was measured after incubation for 40 min at 37 °C, by absorbance at 405 nm.

mRNA isolation and qRT-PCR

Total RNA and miRNA were isolated from cells using miRNeasy Mini kit (Qiagen, Hilden, Germany) according to the manufacturer's instructions. For mRNA, cDNA synthesis was carried out with the Revert Aid H Minus First Strand cDNA Synthesis Kit (Fermentas, St Leon-Rot, Germany). The average Ct value of the housekeeping genes *HPRT1* and *GAPDH* was used for normalization of mRNA analysis. Primers' sequences are provided in Supplementary Table S8. The miRNA Reverse Transcription kit, miRNA specific primer sets for miR-206 and RNU48, as well as the TaqMAN Fast Universal PCR Master Mix (2 ×), were from Invitrogen. The Ct value of RNU48 was used for normalization of miR-206 expression analysis. All qPCR reactions were performed using an ABI Prism 7900HT Sequence Detection System (Applied Biosystems, Weiterstadt, Germany). The relative gene expression level of one gene compared with control was given by the following equation: fold expression level = $2^{-\Delta\Delta Ct}$.

Tube formation assay

For capillary-like tube formation assays, 1×10^5 human vein endothelial cells (HUVECs) were incubated on Matrigel (BD Biosciences, Bedford, MA, USA) in EBM-2 medium with a mixture of EBM-2 and 25% conditioned medium in well plates for 6 h ($n = 6$ fields/group). Images were photographed by light microscopy (Nikon, Danderyd, Sweden). Tube numbers were analyzed using Adobe Photoshop CS5.

Animal studies

Approximately 5×10^6 of PANC-1 tumor cells or PANC10.05 cells were subcutaneously injected into the back along the mid-dorsal line of 4-week-old SCID mice. Tumor volumes were measured two to three times per week and were calculated according to the standard formula (volume = length × width × width × 0.52). PANC-1-formed tumors were *in vivo* transfected weekly with a mixture of 10 μg of *mir*Vana miR-206 mimics or miRNA-negative control (Ambion) and *in vivo*-jet PEI (Polyplus, NY, USA) in 0.015% collagenase II (Sigma) solution intratumorally when tumor size had reached 0.2 cm^3. Mice were killed 7 days after the last intratumoral injection using a lethal dose of CO_2. All animal studies were approved by the Northern Stockholm Experimental Animal Ethical Committee.

Immunohistochemistry

Immunohistochemical staining of whole-mount tissue samples was performed. Tumor tissues were fixed with 4% paraformaldehyde overnight and cut into small pieces. Tissues were digested at room temperature with 20 mM proteinase K in 10 mM Tris buffer (pH 7.5) for 5 min, followed by incubation in 100% methanol for 30 min. Tissues were washed with PBS and incubated overnight at 4 °C in PBS containing 3% skim milk in 0.3% Triton X-100, followed by incubation with the indicated combinations of a rat monoclonal anti-mouse CD31 (1:200; BD-Pharmingen, Bedford, MA, USA) and a rabbit polyclonal anti-LYVE-1 (1:200; AngioBio, Del Mar, CA, USA). Samples were thoroughly rinsed, and blood as well as lymph vessels were detected using fluorescently labeled secondary antibodies of Alexa Fluor 555-labeled goat anti-rat (1:200; Invitrogen), and Cy5-labeled goat anti-rabbit (1:200; Millipore, Billerica, MA, USA), respectively. After washing, tissues were mounted using Vectashield mounting medium (Vector Laboratories, Burlingame, CA, USA) and were analyzed by confocal microscopy (Nikon C1 Confocal microscope, Nikon Corporation, Japan).

Statistical analysis

Data are presented as mean ± s.d., unless indicated differently. Samples were analyzed by unpaired two-tailed student's *t*-test, unless mentioned otherwise and *P*-values < 0.05 were considered as being statistically significant. *P*-values < 0.05, < 0.01 and < 0.001 are indicated with one, two and three asterisks, respectively.

CONFLICT OF INTEREST

The authors declare no conflict of interest.

ACKNOWLEDGEMENTS

We thank Prof George Mosialos and Dr Joerg Hoheisel for kindly providing us with the 3xKBL and pCMV-p65 vectors, and the BxPC-3, MiaPaca-2, Colo357, Capan-1 and CFPAC-1 cell lines, respectively. We thank Dr Christoph Roesli for providing us with the HPNE and HPDE cell lines and the DKFZ Genomics and Proteomics Core Facility for performing excellent services. This work was supported with funding from the German Federal Ministry of Education and Research (NGFN grant 01GS0816) and the Deutsche Forschungsgemeinschaft (DIP project WI3499/1-1).

REFERENCES

1 Siegel R, Naishadham D, Jemal A. Cancer statistics, 2012. *CA Cancer J Clin* 2012; **62**: 10–29.
2 Tuveson DA, Hingorani SR. Ductal pancreatic cancer in humans and mice. *Cold Spring Harb Symp Quant Biol* 2005; **70**: 65–72.
3 Warshaw AL, Fernandez-del Castillo C. Pancreatic carcinoma. *N Engl J Med* 1992; **326**: 455–465.
4 Hingorani SR, Petricoin EF, Maitra A, Rajapakse V, King C, Jacobetz MA *et al.* Preinvasive and invasive ductal pancreatic cancer and its early detection in the mouse. *Cancer Cell* 2003; **4**: 437–450.
5 Aguirre AJ, Bardeesy N, Sinha M, Lopez L, Tuveson DA, Horner J *et al.* Activated Kras and Ink4a/Arf deficiency cooperate to produce metastatic pancreatic ductal adenocarcinoma. *Genes Dev* 2003; **17**: 3112–3126.
6 Ying H, Elpek KG, Vinjamoori A, Zimmerman SM, Chu GC, Yan H *et al.* PTEN is a major tumor suppressor in pancreatic ductal adenocarcinoma and regulates an NF-kappaB-cytokine network. *Cancer Discov* 2011; **1**: 158–169.
7 Wang W, Abbruzzese JL, Evans DB, Larry L, Cleary KR, Chiao PJ. The nuclear factor-kappa B RelA transcription factor is constitutively activated in human pancreatic adenocarcinoma cells. *Clin Cancer Res* 1999; **5**: 119–127.
8 Arlt A, Gehrz A, Muerkoster S, Vorndamm J, Kruse ML, Folsch UR *et al.* Role of NF-kappaB and Akt/PI3K in the resistance of pancreatic carcinoma cell lines against gemcitabine-induced cell death. *Oncogene* 2003; **22**: 3243–3251.

9 Fujioka S, Sclabas GM, Schmidt C, Frederick WA, Dong QG, Abbruzzese JL *et al.* Function of nuclear factor kappaB in pancreatic cancer metastasis. *Clin Cancer Res* 2003; **9**: 346–354.
10 Ling J, Kang Y, Zhao R, Xia Q, Lee DF, Chang Z *et al.* KrasG12D-induced IKK2/beta/NF-kappaB activation by IL-1alpha and p62 feedforward loops is required for development of pancreatic ductal adenocarcinoma. *Cancer Cell* 2012; **21**: 105–120.
11 Esquela-Kerscher A, Slack FJ. Oncomirs—microRNAs with a role in cancer. *Nat Rev Cancer* 2006; **6**: 259–269.
12 du Rieu MC, Torrisani J, Selves J, Al Saati T, Souque A, Dufresne M *et al.* MicroRNA-21 is induced early in pancreatic ductal adenocarcinoma precursor lesions. *Clin Chem* 2010; **56**: 603–612.
13 Munding JB, Adai AT, Maghnouj A, Urbanik A, Zollner H, Liffers ST *et al.* Global microRNA expression profiling of microdissected tissues identifies miR-135b as a novel biomarker for pancreatic ductal adenocarcinoma. *Int J Cancer* 2012; **131**: E86–E95.
14 Keklikoglou I, Koerner C, Schmidt C, Zhang JD, Heckmann D, Shavinskaya A *et al.* MicroRNA-520/373 family functions as a tumor suppressor in estrogen receptor negative breast cancer by targeting NF-kappaB and TGF-beta signaling pathways. *Oncogene* 2012; **31**: 4150–4163.
15 Donahue TR, Tran LM, Hill R, Li Y, Kovochich A, Calvopina JH *et al.* Integrative survival-based molecular profiling of human pancreatic cancer. *Clin Cancer Res* 2012; **18**: 1352–1363.
16 Hudson RS, Yi M, Esposito D, Watkins SK, Hurwitz AA, Yfantis HG *et al.* MicroRNA-1 is a candidate tumor suppressor and prognostic marker in human prostate cancer. *Nucleic Acids Res* 2012; **40**: 3689–3703.
17 Taulli R, Bersani F, Foglizzo V, Linari A, Vigna E, Ladanyi M *et al.* The muscle-specific microRNA miR-206 blocks human rhabdomyosarcoma growth in xenotransplanted mice by promoting myogenic differentiation. *J Clin Invest* 2009; **119**: 2366–2378.
18 Tavazoie SF, Alarcon C, Oskarsson T, Padua D, Wang Q, Bos PD *et al.* Endogenous human microRNAs that suppress breast cancer metastasis. *Nature* 2008; **451**: 147–152.
19 Liou GY, Doppler H, Necela B, Krishna M, Crawford HC, Raimondo M *et al.* Macrophage-secreted cytokines drive pancreatic acinar-to-ductal metaplasia through NF-kappaB and MMPs. *J Cell Biol* 2013; **202**: 563–577.
20 Hofmann I, Weiss A, Elain G, Schwaederle M, Sterker D, Romanet V *et al.* K-RAS mutant pancreatic tumors show higher sensitivity to MEK than to PI3K inhibition *in vivo*. *PloS One* 2012; **7**: e44146.
21 Sarkar S, Swiercz R, Kantara C, Hajjar KA, Singh P. Annexin A2 mediates up-regulation of NF-kappaB, beta-catenin, and stem cell in response to progastrin in mice and HEK-293 cells. *Gastroenterology* 2011; **140**: 583–95 e4.
22 Zhang G, Schetter A, He P, Funamizu N, Gaedcke J, Ghadimi BM *et al.* DPEP1 inhibits tumor cell invasiveness, enhances chemosensitivity and predicts clinical outcome in pancreatic ductal adenocarcinoma. *PloS One* 2012; **7**: e31507.
23 Campbell PM, Groehler AL, Lee KM, Ouellette MM, Khazak V, Der CJ. K-Ras promotes growth transformation and invasion of immortalized human pancreatic cells by Raf and phosphatidylinositol 3-kinase signaling. *Cancer Res* 2007; **67**: 2098–2106.
24 Zheng L, Foley K, Huang L, Leubner A, Mo G, Olino K *et al.* Tyrosine 23 phosphorylation-dependent cell-surface localization of annexin A2 is required for invasion and metastases of pancreatic cancer. *PloS One* 2011; **6**: e19390.
25 Brownstein C, Deora AB, Jacovina AT, Weintraub R, Gertler M, Khan KM *et al.* Annexin II mediates plasminogen-dependent matrix invasion by human monocytes: enhanced expression by macrophages. *Blood* 2004; **103**: 317–324.
26 Madureira PA, Surette AP, Phipps KD, Taboski MA, Miller VA, Waisman DM. The role of the annexin A2 heterotetramer in vascular fibrinolysis. *Blood* 2011; **118**: 4789–4797.
27 Keane MP, Belperio JA, Xue YY, Burdick MD, Strieter RM. Depletion of CXCR2 inhibits tumor growth and angiogenesis in a murine model of lung cancer. *J Immunol* 2004; **172**: 2853–2860.
28 Matsuo Y, Raimondo M, Woodward TA, Wallace MB, Gill KR, Tong Z *et al.* CXC-chemokine/CXCR2 biological axis promotes angiogenesis *in vitro* and *in vivo* in pancreatic cancer. *Int J Cancer* 2009; **125**: 1027–1037.
29 Miyake M, Goodison S, Urquidi V, Gomes Giacoia E, Rosser CJ. Expression of CXCL1 in human endothelial cells induces angiogenesis through the CXCR2 receptor and the ERK1/2 and EGF pathways. *Lab Invest* 2013; **93**: 768–778.
30 Wang D, Wang H, Brown J, Daikoku T, Ning W, Shi Q *et al.* CXCL1 induced by prostaglandin E2 promotes angiogenesis in colorectal cancer. *J Exp Med* 2006; **203**: 941–951.
31 Bussolino F, Wang JM, Defilippi P, Turrini F, Sanavio F, Edgell CJ *et al.* Granulocyte- and granulocyte-macrophage-colony stimulating factors induce human endothelial cells to migrate and proliferate. *Nature* 1989; **337**: 471–473.
32 Pylayeva-Gupta Y, Lee KE, Hajdu CH, Miller G, Bar-Sagi D. Oncogenic Kras-induced GM-CSF production promotes the development of pancreatic neoplasia. *Cancer Cell* 2012; **21**: 836–847.
33 Yang L, DeBusk LM, Fukuda K, Fingleton B, Green-Jarvis B, Shyr Y *et al.* Expansion of myeloid immune suppressor Gr+CD11b+ cells in tumor-bearing host directly promotes tumor angiogenesis. *Cancer Cell* 2004; **6**: 409–421.
34 Bergers G, Brekken R, McMahon G, Vu TH, Itoh T, Tamaki K *et al.* Matrix metalloproteinase-9 triggers the angiogenic switch during carcinogenesis. *Nature Cell Biol* 2000; **2**: 737–744.
35 Stamatovic SM, Keep RF, Mostarica-Stojkovic M, Andjelkovic AV. CCL2 regulates angiogenesis via activation of Ets-1 transcription factor. *J Immunol* 2006; **177**: 2651–2661.
36 Low-Marchelli JM, Ardi VC, Vizcarra EA, van Rooijen N, Quigley JP, Yang J. Twist1 induces CCL2 and recruits macrophages to promote angiogenesis. *Cancer Res* 2013; **73**: 662–671.
37 Stahlhut C, Suarez Y, Lu J, Mishima Y, Giraldez AJ. miR-1 and miR-206 regulate angiogenesis by modulating VegfA expression in zebrafish. *Development* 2012; **139**: 4356–4364.
38 Cao R, Ji H, Feng N, Zhang Y, Yang X, Andersson P *et al.* Collaborative interplay between FGF-2 and VEGF-C promotes lymphangiogenesis and metastasis. *Proc Natl Acad Sci USA* 2012; **109**: 15894–15899.
39 Skobe M, Hawighorst T, Jackson DG, Prevo R, Janes L, Velasco P *et al.* Induction of tumor lymphangiogenesis by VEGF-C promotes breast cancer metastasis. *Nat Med* 2001; **7**: 192–198.
40 Tammela T, Alitalo K. Lymphangiogenesis: molecular mechanisms and future promise. *Cell* 2010; **140**: 460–476.
41 Cao Y. Opinion: emerging mechanisms of tumour lymphangiogenesis and lymphatic metastasis. *Nat Rev Cancer* 2005; **5**: 735–743.
42 Sharma M, Blackman MR, Sharma MC. Antibody-directed neutralization of annexin II (ANX II) inhibits neoangiogenesis and human breast tumor growth in a xenograft model. *Exp Mol Pathol* 2012; **92**: 175–184.
43 Wang CY, Chen CL, Tseng YL, Fang YT, Lin YS, Su WC *et al.* Annexin A2 silencing induces G2 arrest of non-small cell lung cancer cells through p53-dependent and -independent mechanisms. *J Biol Chem* 2012; **287**: 32512–32524.
44 Seckinger A, Meissner T, Moreaux J, Depeweg D, Hillengass J, Hose K *et al.* Clinical and prognostic role of annexin A2 in multiple myeloma. *Blood* 2012; **120**: 1087–1094.
45 Stupack DG, Cheresh DA. ECM remodeling regulates angiogenesis: endothelial integrins look for new ligands. *Sci STKE* 2002; **2002**: pe7.
46 Singh A, Happel C, Manna SK, Acquaah-Mensah G, Carrerero J, Kumar S *et al.* Transcription factor NRF2 regulates miR-1 and miR-206 to drive tumorigenesis. *J Clin Invest* 2013; **123**: 2921–2934.
47 Hanahan D, Weinberg RA. Hallmarks of cancer: the next generation. *Cell* 2011; **144**: 646–674.

Supplementary Information accompanies this paper on the Oncogene website (http://www.nature.com/onc)